

CHARACTERIZATION OF AXIAL FLOW IMPELLERS IN PULP FIBRE SUSPENSIONS

M. Bhole, C. Ford and C.P.J. Bennington*

*Department of Chemical and Biological Engineering, University of British Columbia
2360 East Mall, Vancouver, BC, V6T 1Z3 Canada; e-mail: cpjb@chml.ubc.ca*

Abstract. Two axial flow impellers commonly used in pulp agitation applications were characterized in hardwood and softwood low-consistency pulp fibre suspensions. The impellers operated in the laminar and transition-to-turbulence regimes with the suspension mass concentration significantly affecting both power and axial thrust numbers. Axial force numbers could be collapsed to a single operating curve using the yield stress Reynolds number, but the power number remained a function of suspension properties. CFD was used to model impeller flow using a Bingham approximation to describe the suspension rheology. Model agreement with the experimental measurements was generally good, with the values of N_p and N_f determined to within 24% and 16%, respectively. The error can be explained by the uncertainty in the rheological characterization of the pulp suspension, particularly the yield stress.

Key words: Mixing; Pulp fibre suspensions; Yield stress; Axial flow impellers; CFD

1. INTRODUCTION

Mixing is an essential operation in pulp and paper manufacture. Pulp fibre suspensions are non-Newtonian and possess a yield stress. They must be uniformly blended with other pulp streams and with additives, fillers and chemicals prior to papermaking. The required mixing is commonly accomplished in mechanically stirred vessels (stock chests) using axial flow impellers designed for high flow, such as marine impellers, the Maxflo (Chemineer Inc., Dayton, USA) and the A312 (Lightnin Inc., Rochester, USA).

Stock chest design involves selecting the correct impeller and power input required to ensure complete motion through a specified chest volume. Due to suspension rheology this can be a challenge even at low suspension mass concentrations ($C_m = 2$ to 4%). Chest design is based on proprietary criteria but typically follows the method summarized by Yackel [1] which matches the fluid momentum generated by an impeller with that needed to provide complete motion over the suspension surface in the chest. The later is determined from correlations developed for a wide range of variables, including chest geometry (typically rectangular), fibre type and suspension concentration. The impeller momentum flux or momentum number, Mo , is given by

$$Mo = CN^2D^4 \quad (1)$$

where C is a constant that depends on impeller geometry and N and D are the impeller speed and diameter, respectively. C is usually available from the impeller manufacturer, often based on tests made in water. Yackel [1] tabulates Mo values for several impellers over a range of operating conditions for use with his design procedure.

Axial flow impellers are most often characterized by their power number, N_p , and more recently by their axial force number, N_f

$$N_p = \frac{P}{\rho N^3 D^5} \text{ where } P = 2\pi NM \text{ and } N_f = \frac{F_A}{\rho N^2 D^4} \quad (2)$$

with P being the power drawn, M the shaft torque and F_A the axial thrust. N_p for mixing of Newtonian fluids in standard vessels is available in the literature as a function of Reynolds number. For non-Newtonian fluids, the methodology developed by Metzner and Otto can be used to determine the appropriate Reynolds number for these correlations [2–4]. N_f has not been widely adopted for mixer design although Yackel's method essentially employs it. However, Yackel's procedure has been shown to underestimate the power required for effective mixing of pulp suspensions [5]. Indeed, even when complete surface motion is attained, stagnant zones exist below the suspension surface which reduces mixing efficiency.

The mixing of yield stress fluids results in formation of a cavern around the impeller where fluid motion is localized. Outside the cavern, fluid stresses fall below the yield stress and the fluid is stagnant [6,7]. Cavern size can be estimated by balancing the force transferred from the impeller to the cavern boundary once a cavern shape has been specified. A number of researchers have done this [7–9], and Amanullah *et al.* [9] included both N_p and N_f in their equation for determining the surface area, A_s , of an unbounded spherical cavern created by an axial flow impeller,

$$A_s = \text{Re}_y D^2 \sqrt{N_f^2 + \left(\frac{4N_p}{3\pi}\right)^2} \quad (3)$$

where the yield stress Reynolds number, Re_y , is given by

$$\text{Re}_y = \frac{\rho N^2 D^2}{\tau_y} \quad (4)$$

with τ_y the suspension yield stress. When the parameters (N_f and N_p) chosen for Eqn. 3 correspond to the actual mixer operating conditions (rather than values determined under turbulent conditions) the predictions are more accurate [9]. Since the rheological behavior of pulps suspensions is not well characterized the measurement of these parameters becomes imperative. We have done this for two common axial flow impellers under typical pulp suspension mixing conditions.

Computational fluid dynamics (CFD) has emerged as a powerful tool for characterizing impeller behaviour. While most simulations have focused on mixing single-phase Newtonian fluids under turbulent conditions, some more recent approaches have modeled agitation in non-Newtonian fluids [10–13]. Although these simulations provide information on velocity profiles and permit identification of regions of poor mixing, their accuracy depends significantly on the characterization of the fluid rheology [14]. We have used a commercial CFD package to determine impeller parameters under relevant pulp mixing conditions and compared them with our experimental measurements to determine the accuracy of this approach.

2. EXPERIMENTAL

The primary vessel used for impeller characterization (T1) is a fully baffled (four baffles of width $B = 2.5$ cm), slightly tapered, cylindrical vessel with diameter varying linearly from 29 cm at the top of the vessel to 26 cm at the bottom as shown in Fig. 1. Suspension height was

maintained at $Z = 29$ cm. Impellers were mounted on an instrumented shaft driven by a 0.25 kW variable speed motor with the impeller off-bottom clearance, C_1 , maintained at 10 cm. Two impeller types were studied: a standard marine impeller (3-bladed, $D = 9.0$ cm, pitch ratio = 1.5) and a series of geometrically scaled Maxflo impellers (Chemineer Inc., Dayton, OH) (3 bladed, $D = 10.2, 14.0$ and 16.5 cm; pitch ratio = 0.44). Photographs of the impellers are included in Fig. 1. Impeller rotational speed was measured to ± 1 rpm using an optical tachometer and shaft torque was measured to ± 0.002 N·m using an in-line strain gauge. The axial force was measured gravimetrically using a balance (Mettler Toledo SB32001) accurate to ± 0.1 g although variations in axial force due to shaft vibrations at high rotational speeds could be as high as ± 20 g. Tests were made in the down-pumping mode with impeller speed varied from 50 to 800 rpm.



Fig. 1: Mixing vessel (T1) and impellers studied (Maxflo on the left and the marine impeller on the right)

Two industrial pulp fibre suspensions were studied. A softwood bleached kraft pulp (SW) with a length-weighted fibre length, l_f , of 2.96 mm and a hardwood bleached kraft (HW) with $l_f = 1.28$ mm were obtained from Domtar Inc. (Windsor, QC). Suspension mass concentration was varied from $C_m = 0$ to 4% with the suspension yield stress measured using a Haake RV12 viscometer giving the following correlations

$$\tau_y = 12.3C_m^{2.05} \text{ for the softwood pulp} \quad (5)$$

$$\tau_y = 1.25C_m^{3.00} \text{ for the hardwood pulp} \quad (6)$$

with the coefficient of variation in yield stress averaging $\pm 22\%$ over the mass concentration range, in line with past measurements [15].

3. RESULTS AND DISCUSSION

3.1 Impeller Characterization

N_P and N_f for agitation of softwood pulp suspensions with a Maxflo impeller ($D = 10.2$ cm) and the marine impeller are shown in Figs 2 and 3 (plotted against impeller rotational speed, N). For both impellers, the dependence of N_f and N_P on N indicate that flow is in the laminar and transition-to-turbulence regimes. For a fixed rotational speed, both N_f and N_P increase with suspension consistency indicating a significant influence of suspension rheology on impeller performance. For a given impeller speed and suspension consistency, the N_f and N_P for the marine propeller are higher than for the Maxflo impeller due to its higher pitch ratio.

N_P and N_f were measured in both hardwood and softwood pulp suspensions from $C_m = 1$ to 4% and are plotted against Re_y in Fig. 4. For N_f all curves collapse to a single operating line. However, the same is not true for N_P where suspension properties other than the suspension yield stress affect the power number. Similar results are reported for pulp suspensions by Ein-Mozaffari *et al.* [16] and for Bingham plastic fluids by Nagata [17].

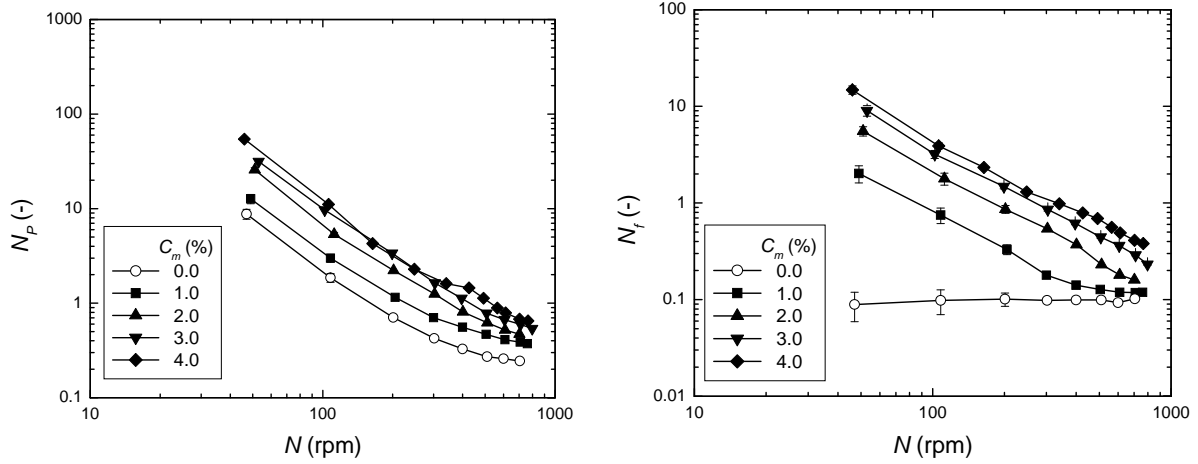


Fig. 2: N_P and N_f for Maxflo impeller ($D = 10.2$ cm) in softwood pulp suspensions

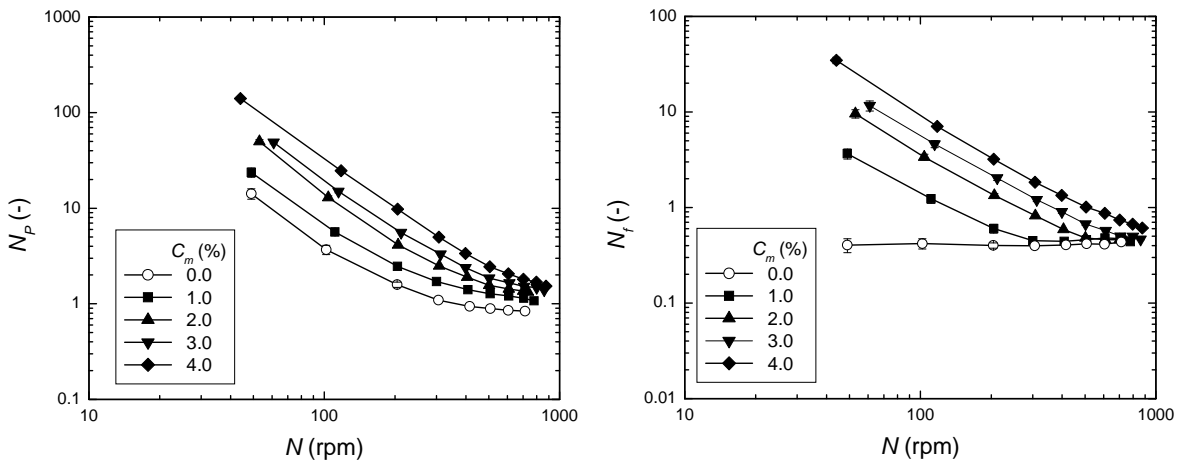


Fig. 3: N_P and N_f for marine impeller ($D = 9.0$ cm) in softwood pulp suspensions

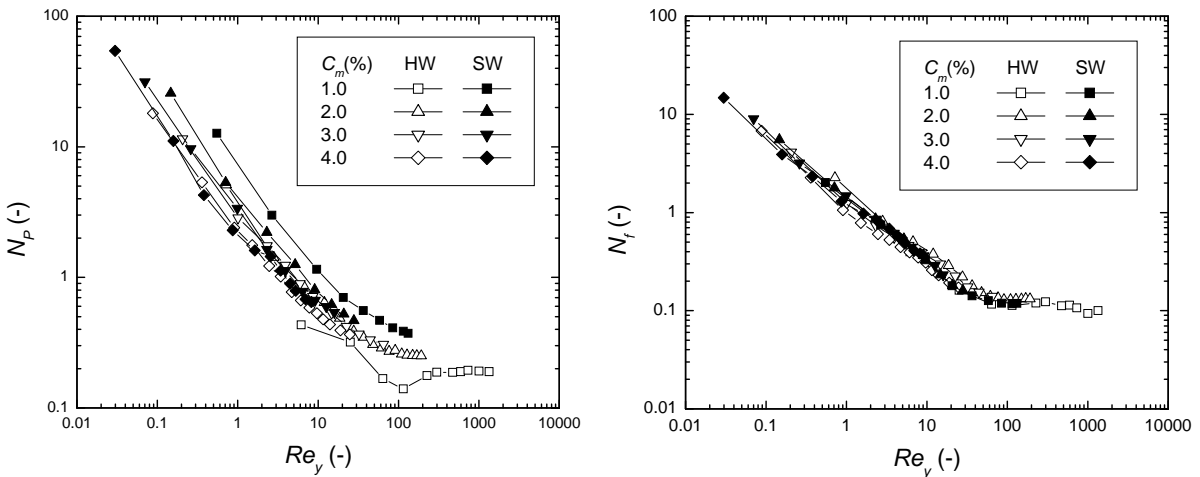


Fig. 4: N_P and N_f for Maxflo Impeller ($D = 10.2$ cm) in hardwood and softwood pulp suspensions.

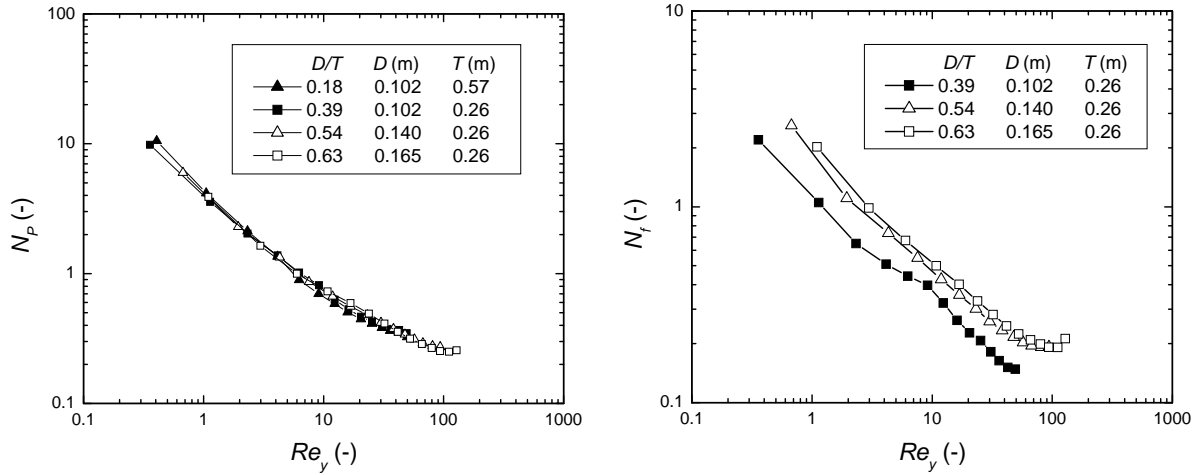


Fig. 5: N_p and N_f for Maxflo impellers as a function of D/T in hardwood pulp suspensions.

The effect of scale-up was studied by measuring N_p and N_f as a function of Re_y for various D/T ratios in a $C_m = 3\%$ hardwood pulp suspension using the Maxflo impeller. Vessel T1 was used for most tests in addition to a larger cylindrical baffled vessel (T2) having $T = 57$ cm which allowed D/T to be varied from 0.18 to 0.60. Figure 5 shows that N_p is almost independent of D/T over the range considered. In Newtonian fluids N_p is a function of D/T for axial flow impellers because the flow generated interacts with the vessel walls (and changes as D/T changes [18]). In pulp suspensions, the cavern created around the impeller often does not reach the vessel walls and thus no significant effect of D/T is observed. N_f does depend on D/T and further study is needed to quantify the effect.

So far we have presented results for cylindrical baffled tanks. Industrial stock chests are usually rectangular due to space constraints and the ease of construction. Consequently some tests were made in a square tank (S1) with $T = Z = 24$ cm. N_p and N_f for the $D = 10.2$ cm Maxflo impeller in a $C_m = 3\%$ hardwood pulp suspension did not vary significantly (less than a 10% change) from the values measured in the cylindrical vessel (T1).

3.2 Impeller Characterization using CFD

Characterization of impellers for different fluid/suspensions can be expensive and time consuming. In this regard, using CFD to model impeller performance is promising. We used the commercial CFD software package, Fluent V6.3 (Fluent Inc., Lebanon, NH) to simulate the experimental tests performed using the $D = 10.2$ cm Maxflo impeller in a $C_m = 3\%$ hardwood suspension in vessel T1. The computational domain within the vessels was discretized with multi-block mesh structures using Gambit software (v. 2.4.6, Fluent, Lebanon, NH) with cell density optimized to capture flow details without being excessive. Increased mesh resolution was used near all solid boundaries with increases in mesh size limited to a growth rate of 20% [19].

A modified Herschel-Bulkley model was used to describe suspension rheology. Below the yield stress, the suspension was modeled as an extremely viscous fluid, μ_o

$$\mu = \mu_o \text{ for } \tau \leq \tau_y \quad (7)$$

Above the yield stress, the apparent viscosity was given by

$$\mu = \frac{\tau_y + k \left[\dot{\gamma}^n - \left(\frac{\tau_y}{\mu_o} \right)^n \right]}{\dot{\gamma}} \text{ for } \tau > \tau_y \quad (8)$$

with the consistency index, k , set to 0.001 Pa·s (the viscosity of water) and the power-law index, n , set to 1.0. The yield stress of the 3 % hardwood suspension was set to its measured value of $\tau_y = 30$ Pa and the yielding viscosity to $\mu_o = 100$ Pa·s [14].

The final three-dimensional mesh of the cylindrical vessel (T1) had 463,742 computational cells. The multiple reference frame approach was used for computation, with coupling between reference frames made using a velocity transformation. A no-slip condition was set at all solid/suspension boundaries and a free slip condition was set at the air/suspension interface.

Mass and momentum conservation equations were solved in the laminar regime using a second order upwind scheme to limit numerical diffusion. For all the conditions simulated, the non-Newtonian Reynolds numbers defined by Attwood and Gibbon [20] and Blasinski and Rzycki [21] were below 10^3 indicating laminar or transitional flow, in agreement with the measured behavior (Figs. 2 and 3). Iterations were continued until the root mean square scaled residuals for each transport equation fell below 1×10^{-6} , with convergence of axial velocity at three different point locations (one near the impeller and two remote from the impeller) monitored to verify that a steady value was reached. Grid independence was verified by demonstrating that further cell refinement near the impeller did not change the computed torque at the impeller center by more than 2% and that the magnitude of velocity calculated at two lines located in the impeller discharge did not change by more than 3%.

The calculated velocity field is shown in Fig. 6 at the vessel mid-plane for geometry T1 at three different impeller speeds. Only vectors having magnitudes below 0.05 m/s are plotted. Regions having velocity >0.05 m/s indicate rapid motion in the impeller (cavern) region and are left blank for clarity. The regions in blue (low velocity) are essentially stagnant. As impeller speed increases, the size of the cavern increases. Note that even at high impeller speeds the cavern does not significantly interact with the vessel walls.

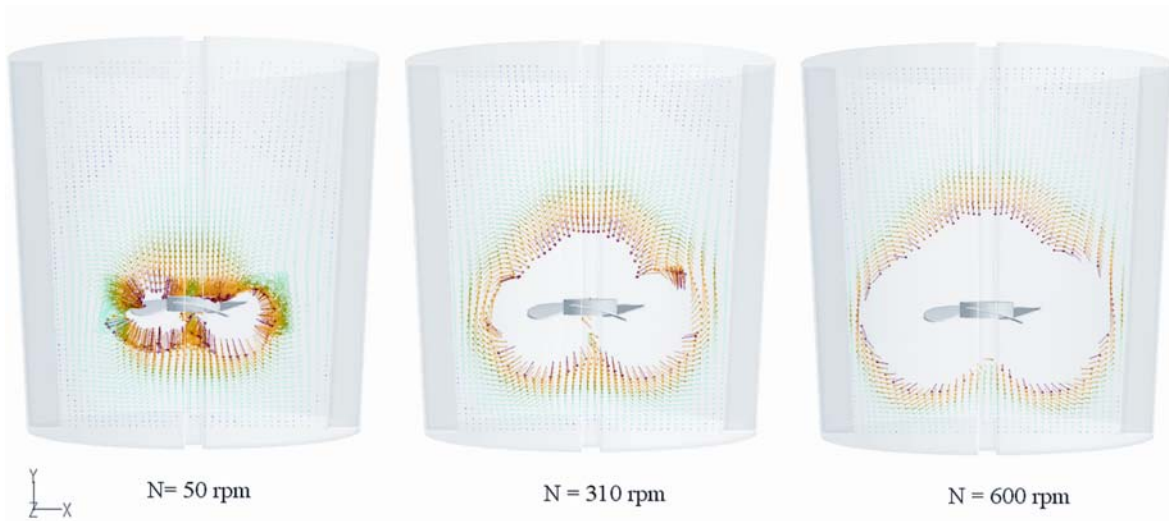


Fig. 6: Velocity vectors colored by velocity magnitude (m/s) at plane $z=0$. Hardwood pulp at $C_m = 3\%$

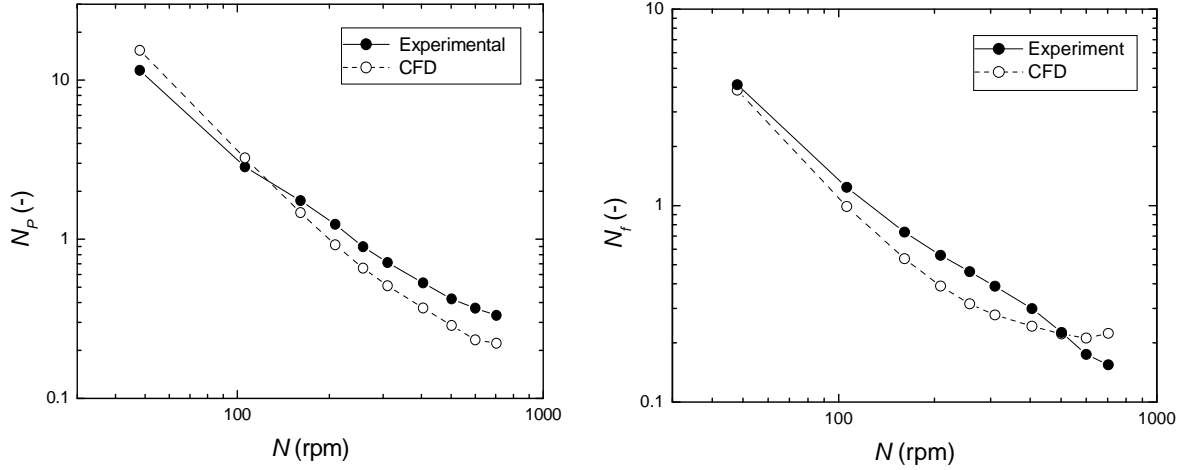


Fig. 7: Comparison of N_p and N_f for experimental and computational tests for cylindrical vessel T1. $D = 10.2$ cm Maxflo impellers in a $C_m = 3\%$ hardwood pulp suspensions as a function of rotational speed.

Measured N_p vs. N and N_f vs. N curves are compared with those obtained from the CFD simulations in Fig. 7 for a $C_m = 3\%$ hardwood suspension in cylindrical vessel T1. Computed values of the shaft torque and the axial thrust acting on the impeller were used in Eqn. 2 to calculate N_p and N_f . The agreement between experimental and computed curves is generally very good over the entire impeller speed range. N_p is under-predicted by 24% except at the lower impeller speeds (13% deviation). N_f is under-predicted by 16%. Computations made for the square vessel (S1) show the same behaviour. The computed values of N_f were very similar for both geometries (within 4%), in agreement with the experimental results.

The fluid forces and torque are calculated using the pressure and velocity fields in the impeller which depend on the boundary conditions and material properties specified for the simulation, particularly the suspension viscosity. In the impeller vicinity, shear rates are high and the viscosity of the suspension is calculated with Eqn. 8 using parameters τ_y , μ_0 , k and n . The calculated viscosity is sensitive to τ_y , which is only measured to an accuracy of $\pm 17\%$ for the $C_m = 3\%$ hardwood suspension, equivalent to ± 5 Pa. Consequently, the estimated viscosity near the impeller is only accurate to $\pm 17\%$ when all other parameters are known with total confidence (which they aren't). When this uncertainty is considered, the deviation between the calculated and measured impeller parameters can be explained.

4. SUMMARY AND CONCLUSIONS

Two axial flow impellers used for the agitation of pulp fibre suspensions were characterized in hardwood and softwood pulp suspensions at low mass concentrations. The impellers operated in the laminar and transition-to-turbulence regimes in the suspensions, with the suspension mass concentration significantly affecting both power and axial thrust numbers. The axial force numbers could be collapsed to a single operating curve using the yield stress Reynolds number, although the power number remained a function of suspension properties. Computational fluid dynamics (Fluent) was used to model impeller flow using a Bingham approximation to describe the suspension rheology. The agreement of the CFD computations was good, with the values of N_p and N_f determined to within 24% and 16% of the experimentally measured values. The discrepancy was attributed primarily to the uncertainty in measuring the suspension yield stress, which was to $\pm 17\%$ for the hardwood suspension at $C_m = 3\%$.

5. ACKNOWLEDGEMENTS

The financial support of NSERC/FP Innovations (Paprican) and the Dynamic Mixing Industrial group is gratefully acknowledged. Thanks to Chemineer Inc. for supplying the Maxflo impellers and to Domtar Inc. for supplying the pulp.

6. REFERENCES

1. Yackel D.C., 1990, *Pulp and Paper Agitation: The History, Mechanics, and Process*, TAPPI Press, Atlanta.
2. Metzner A.B., Otto R.E., 1957, "Agitation of non-Newtonian fluids", *AIChE J.*, **3**, 3-10.
3. Bakker A. and Gates L.E., 1995, "Properly choose mechanical agitators for viscous liquids", *Chem. Eng. Prog.*, **91**, 25-34.
4. Shekhar S.M., Jayanti S., 2003, "Mixing of power law fluids using anchors: Metzner-Otto concept revisited", *AIChE J.*, **49**, 30-40.
5. Ein-Mozaffari F., Bennington C.P.J., Dumont G.A., 2004, "Dynamic mixing in agitated industrial pulp chests", *Pulp & Pap. Can.* **105**, 41-45.
6. Wichterle K, Wein O., 1981, "Threshold of mixing of non-Newtonian liquids", *Int. Chem. Eng.*, **21**, 116-120.
7. Solomon J., Elson T.P., Nienow A.W., Pace G.W., 1981, "Cavern sizes in agitated fluids with a yield stress", *Chem. Eng. Commun.*, **11**, 143-164.
8. Elson T.P., Cheesman D.J., Nienow A.W., 1986, "X-ray studies of cavern sizes and mixing performance with fluids possessing a yield stress", *Chem. Eng. Sci.*, **41**, 2555-2562.
9. Amanullah A., Hjorth S.A., Nienow A.W., 1998, "A new mathematical model to predict cavern diameters in highly shear thinning, power law liquids using axial flow impellers", *Chem. Eng. Sci.*, **53**, 455-469.
10. Kelly W. Gigas B., 2003, "Using CFD to predict the behavior of power law fluids near axial-flow impellers operating in the transitional regime", *Chem. Eng. Sci.*, **58**, 2141-2152.
11. Arratia P.E., Kukura J, Lacombe J., Muzzio F.J., 2006, "Mixing of shear thinning fluids with yield stress in stirred tanks", *AIChE J.*, **52**, 2310-2322.
12. Adams L.W., Barigou M., 2007, "CFD analysis of caverns and pseudo-caverns developed during mixing of non-Newtonian fluids", *Chem. Eng. Res. Des.*, **85**, 598-604.
13. Ford C., Ein-Mozaffari F., Bennington C.P.J., Taghipour F., 2006, "Simulation of mixing dynamics in agitated pulp stock chests using CFD", *AIChE J.*, **52**, 3562-3569.
14. Ford, C., Bennington C.P.J., Taghipour F., 2007, "Modelling a pilot-scale pulp mixing chest using CFD", *J. Pulp Pap. Sci.*, **33**, 115-120.
15. Bennington C.P.J., Kerekes R.J., Grace J.R., 1990, "The yield stress of fibre suspensions", *Can. J. Chem. Eng.*, **68**, 748-757.
16. Ein-Mozaffari F., Dumont G.A., Bennington C.P.J., 2003, "Performance and design of agitated pulp stock chests", *Appita J.*, **56**, 127-133.
17. Nagata S. 1975, *Mixing: principles and applications*, Wiley, New York.
18. Chapple D., Kresta S.M., Wall A., Afacan A. 2002, "The effect of impeller and tank geometry on power number for a pitched blade turbine", *Chem. Eng. Res. Des.*, **80**, 364-372.
19. Fluent 6.3, 2006, "User's guide documentation", Fluent Inc. Lebanon, NH.
20. Attwood D., Gibbon J.D., 1963, "The agitation of paper stock", *Pap. Tech*, **4**, 54-62.
21. Blasinski H., Rzycki E. 1972, "Mixing of non-Newtonian liquids: 2. Power consumption for fibrous suspensions", *Inzh. Chem.*, **2**, 169-182.